Sampling Pulses for Optimal Timing

Abdelkader Bousselham and Christian Bohm, *Member, IEEE*

***Abstract*—When extracting unknown band-limited pulses from sampled data, the Nyquist criterion defines the minimum sampling frequency. With well-defined pulse shapes and a stationary noise environment one can use matched filters to recover time and amplitude, but this is usually not the case with scintillation detectors. If the noise is not stationary other methods must be used. Our study investigates different timing strategies and how the timing precision depends on ADC resolution and sample rate. It also compares the timing precision with data obtained from an analogue setup. Pulses from an LSO crystal with photomultiplier readout are studied experimentally. Our best method gives in this case a 10% improvement in timing compared to a matched filter approach. Some simulation results are also reported.**

***Index Terms*—Analog-digital conversion, digital signal processing, sampling methods, timing.**

I. Introduction

WHEN processing pulses from radiation detectors in physical or medical applications, time and energy are usually the only parameters of interest. While older detection systems used analogue circuitry to process signals before digitization, state-of-the-art detection systems often rely on early digitization, sampling the signals with free running clocks [1]. Digitization is performed after applying a simple analogue filter, usually a low pass filter. Subsequent digital processing is then used to recover time, amplitude and pulse quality information. The latter reveals if the time and amplitude information are compromised by pile-up.

Signal processing in an analogue timing system can be implemented in a free running digital system, provided the sampling rate and sampling precision are sufficiently high. A combination consisting of a pulse shaper and a constant fraction discriminator (CFD) can be shown to be equivalent to an analogue anti-aliasing (low-pass) filter followed by a sampling ADC, a digital filter and a maximum-finder (or zero-crossing). However, apart from parameters equivalent to those in analogue systems, a digital system has additional degrees of freedom with respect to choice of algorithms and filter parameters. More degrees of freedom must necessarily translate into better optimum performance, but whether the improvement is sufficient to motivate the increased complexity must be verified.

Another advantage of digital processing is better treatment of pile-up events. The analogue solution is to shorten the pulses, which means losing statistical information. This is not necessary in a digital system since one can treat normal and pile-up pulses differently, optimizing the approach to match the pulse type.

When extracting unknown band-limited pulses from sampled data, the Nyquist criterion defines the minimum sample rate that does not cause aliasing. In the time domain this can rather loosely be expressed as a minimum of three sample points on the rising edge of the pulse, since one can show that almost all of the signal power occurs below half of this sampling frequency. The rise time $\mathrm{T_r}$ corresponds to a frequency limit of $1/\mathrm{T_r}$ (such pulses have a "knee" at $0.5/\mathrm{T_r}$ [1] and most of the signal power is below twice this frequency), which according to Nyquist must be sampled with a period less than $\mathrm{T_r}/2$, i.e., more than two sample points on the rising edge.

With well-defined pulse shapes and a noisy environment one can use matched (optimum) filters to recover time and amplitude, but the requirement of stationary noise is not always fulfilled. In that case one has to resort to a more basic statistical approach.

II. Least Square Estimators

A timing algorithm for the non-stationary case must be derived from "first principles", i.e., the maximum likelihood method or equivalently the least square method, if one can assume that the noise is normally distributed. Let us make this assumption here. Let us also assume that the background has already been removed.

Using matrix formalism one can express the least square sum as:

$$\chi^2 = (Y - F(\theta, t))^T V(\theta, t)^{-1} (Y - F(\theta, t)) \qquad (1)$$

where Y is the sampled data, $\mathrm{F}(\boldsymbol{\theta}, \mathrm{t})$ an ideal pulse starting at t and V the covariance matrix, which expresses the noise correlation between nearby data points. In the general case F depends on a set of parameters $\boldsymbol{\theta}$ of which the amplitude (a) is the most important. Other parameters may affect the pulse shape. Let us assume that in this case the influence of the other parameters can be neglected in comparison to a. The task is to estimate t by minimizing (1) and to do that as efficiently as possible with a minimal systematic error. For this we need an accurate pulse description F. As long as V is positive definite (semi-definite can also work), which is the case if V is a covariance matrix, and the noise not too large, we can always find an accurate t-value. χ^2 is minimized if F is close to Y. Actually it is 0 if they are identical. Thus if F is a correct model, (1) will lead to a consistent estimator of the parameters. One can also show that if the noise level is small the estimators are unbiased. However, the precision and thus the efficiency depend on how well we can determine V. This means that even if one erroneously assumes

Manuscript received October 20, 2006; revised December 20, 2006. This work was supported by EC FP6 (Contract LSHC-CT-2004-505785). The publication does not necessarily reflect the views of the EC. The community is not liable for any use that may be made of the information contained herein.

The authors are with the Department of Physics, AlbaNova University Center, Stockholm University, SE-106 91 Stockholm, Sweden (e-mail: kader@physto.se; bohm@physto.se).

Color versions of one or more of the figures in this paper are available online at http://ieeexplore.ieee.org.

Digital Object Identifier 10.1109/TNS.2007.892692

TABLE I
DIFFERENT TIMING ESTIMATORS

	F(a,t)	V(a,t)	amplitude estimator, a	timing estimator, t minimizes
M1	P(t)	V diagonal	1	$-P^TY$
M2	P(t)	V	1	$-P^TV^{-1}Y$
M3	aP(t)	V	$\frac{P^TV^{-1}Y}{P^TV^{-1}P}$	$-P^TV^{-1}P$
M4	aP(t)	V(t)	$\frac{P^TV^{-1}Y}{P^TV^{-1}P}$	$Y^TV^{-1}Y-\frac{\left(P^TV^{-1}Y\right)^2}{P^TV^{-1}P}$
M5	aP(t)	aV(t)	$\sqrt{\frac{Y^TV(t)^{-1}Y}{P(t)^TV(t)^{-1}P(t)}}$	$Y^TV(t)^{-1}Y$
M6	aP(t)	a^2V(t)	$\frac{Y^TV^{-1}Y}{P^TV^{-1}Y}$	$-\frac{\left(P^TV^{-1}Y\right)^2}{P^TV^{-1}Y}$

stationary noise the result will still be accurate, but not as precise as it would be with a correct noise description, provided noise level is not too large.

There are different possibilities to describe the situation. If we know that the pulses are of the same size we can use $\mathrm{P(t)}$ instead of $\mathrm{F}(\boldsymbol{\theta},\mathrm{t})$. If we know that the pulse shape is invariant but the amplitude varies we can use $\mathrm{aP(t)}$.

If the noise can be assumed stationary, V is a band matrix with the same elements across the band. If the noise at the different sample points is uncorrelated we have a diagonal matrix. Other possibilities are that the noise amplitude is proportional to the pulse amplitude, or that the noise is related to a Poisson process. In these cases the proper covariance matrix would be $\mathrm{a^2V(t)}$ or $\mathrm{aV(t)}$, respectively.

Minimizing the χ^2 with respect to the amplitude will give us different amplitude estimators depending on the F and V model we have used. Inserting these models in (1) and minimizing with respect to t will give us a timing estimator (see Table I).

If we take the $\mathrm{aP(t)-V(t)}$ combination we get:

$$\begin{aligned}\chi^2 &= (Y-aP)^TV^{-1}(Y-aP)\\ &= Y^TV^{-1}Y-2aP^TV^{-1}Y+a^2P^TV^{-1}P \qquad (1')\end{aligned}$$

which gives us the following amplitude estimator:

$$\frac{d\chi^2}{da}=0\Rightarrow a=\frac{P^TV^{-1}Y}{P^TV^{-1}P} \qquad (2)$$

Inserting this value in the expression above results in:

$$\begin{aligned}\chi^2 &= Y^TV^{-1}Y-\frac{(P^TV^{-1}Y)^2}{P^TV^{-1}P}\\ &= Y^TV^{-1}Y-(CY)^2. \qquad (3)\end{aligned}$$

The task is now to find the relative position of Y and P that minimizes χ^2. As a start let us consider Y as fixed moving P (and V). In the case of stationary noise minimizing expression (3) is equivalent to matched filter processing, since the first term does not depend on the pulse position and the denominator in the second term is constant.

The expression and its time derivatives are non-linear but can be solved iteratively. An accurate treatment requires a matrix and a scalar multiplication for each iteration, assuming that previously compiled sets of $\mathrm{V^{-1}}$ and C are stored in memory. However, with modern Field Programmable Gate Arrays (FPGA) the metric of real-time computational complexity has changed drastically, making very large real time computational tasks feasible [2]. Another approach is to combine a simplified approximate real time calculation with a detailed treatment up- stream.

With one (P, V) combination the formula above (3) can be used to identify the best positioning (timing) by sliding P relative to Y in steps of sample periods $(\Delta\mathrm{t})$. The same (P, V) combination can be used after modifying the indices. Sub-sample timing, however, requires re-sampling along a delayed grid or sampling the delayed pulse, $(\mathrm{P(t+\Delta tk/n)})$. For sub- sample timing there must thus be as many different V's and C's as there are sub samples (n) in the sample interval $(\Delta\mathrm{t})$. A binary search and a final interpolation can be used for the optimization [2].

Another approach to minimizing (3) is to consider P (and V) stationary, and move Y to find the minimum. To find the sub-sample position will then require interpolation. Sinc-interpolation of Y will introduce no errors provided the initial low pass filter fulfills the Nyquist criteria. A sufficiently precise spline may also work.

Above we assumed that the covariance matrix was independent of the amplitude. However, if the noise is purely Poisson distributed we can show (see (7) below) that V is linearly dependent on a, i.e., $\mathrm{V(a,t)=a\cdot V(1,t)=a\cdot V(t)}$. Thus:

$$\begin{aligned}\chi^2 &= (Y-aP(t))^TV(a,t)^{-1}(Y-aP(t))\\ &= Y^TV(t)^{-1}Y/a-2P(t)^TV(t)^{-1}Y\\ &\quad +aP(t)^TV(t)^{-1}P(t). \qquad (4)\end{aligned}$$

This time minimizing the χ-square with respect to the amplitude gives us:

$$\frac{d\chi^2}{da}=0\Rightarrow a^2=\frac{Y^TV(t)^{-1}Y}{P(t)^TV(t)^{-1}P(t)} \qquad (5)$$

Inserting this in the expression above results in:

$$\begin{aligned}\chi^2 &= 2\sqrt{Y^TV(t)^{-1}Y\cdot P(t)^TV(t)^{-1}P(t)}\\ &\quad -2P(t)^TV(t)^{-1}P(t)\\ &= 2\sqrt{P(t)^TV(t)^{-1}P(t)}\cdot(\sqrt{Y^TV(t)^{-1}Y}\\ &\quad -\sqrt{P(t)^TV(t)^{-1}P(t)}). \qquad (6)\end{aligned}$$

The task is now to find the relative position of Y and P that minimizes χ^2. Since $\mathrm{P(t)}$ and $\mathrm{V(t)}$ move together, i.e., $\mathrm{P(t)^TV(t)^{-1}P(t)}$ is independent of t, $\mathrm{Y^TV(t)^{-1}}$ Y is positive and the square root is monotonous, we realize that minimizing χ^2 is the same as minimizing $\mathrm{Y^TV(t)^{-1}Y}$. We have thus six different algorithms that are valid under different circumstances.

In both cases, accurate information about the pulse shape (P) and the covariance matrix (V) is needed to obtain good timing information. Our direct interest in the present investigation was

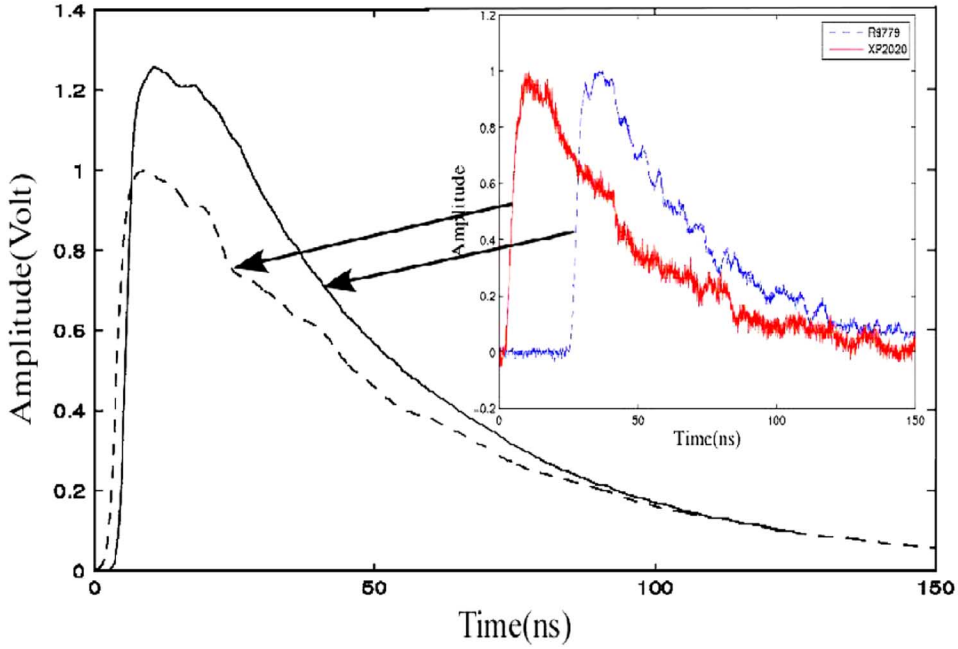

Fig. 1. Average pulses from LSO and XP2020 (dashed) and R9779 (continuous) using 10 000 and 1000 pulses, respectively.

to optimize the timing of gamma-ray detection from LSO scintillator crystals read out by a photomultiplier tube (PMT) for use in a positron camera (PET) application. Therefore, it is for the LSO-PMT combination that we have attempted to estimate P and V. We have done this in different ways: directly from experimental data, by convolving data from a picoseconds light pulse excitation with an exponential or by noise simulations from a detailed pulse model that has been fitted to experimental data. The different approaches are evaluated by comparing the effects on the variance of the gamma coincidence timing of positron annihilations.

III. Experimental Set-Up

Pulses from an LSO-PMT detector combination have been studied experimentally with a LeCroy 8300A oscilloscope with a 3 GHz analogue bandwidth, 20 GS/s sample rate and 8-bit conversion. A PC, which served as an experiment controller, was connected to the oscilloscope via Ethernet. The data was stored on disk for off line analysis using Matlab. The experimental set-up consists of two identical PMTs, each coupled to one of the opposing 4×4 faces of a $4 \times 4 \times 20$ mm LSO crystal. Two different types of PMTs have been used: Photonis XP2020 and Hamamatsu R9779. It was important for the intended digital application that the PMT base circuitry used was linear. The anode signals were fed directly to the oscilloscope. Signals from the last dynode were used to only select pulses belonging to the (450–625) keV energy window.

A reference analogue set-up used a preamplifier, CFD and a TAC (time-to-pulse height-converter). The timing performance of this was 382 ps for XP2020 and 350 ps for the R9779 tube. These are plausible results, indicating that the detector set-up is acceptable.

We have assumed that increasing the sample rate above 20 GS/s and the analogue bandwidth to more than 3 GHz will not significantly improve the timing performance. This assumption is supported by the fact that we have seen that decreasing these values by 50% does not significantly affect the timing precision. This means that most of the information, i.e., the upper frequency limit of the signal, is well below 3 GHz. However, at this point we cannot be sure whether the 8-bit ADC resolution is sufficient. By aligning and averaging digitized pulses we could find an "ideal" pulse shape with better precision (Fig. 1). The alignment was done in different ways, by aligning the maxima of the cross correlations with a reasonable reference pulse shape or by using a Digital version of CFD, i.e., DCFD. Even if we iterated the correlation procedure several times using the aligned averaged as a new reference pulse, constant fraction gave the best result. The reason was that the correlation method is more sensitive to coherent noise, which was present at low level. We also tried Digital Leading Edge Timing (DLET), which, in our case, proved to be inferior to CFD due to noise correlation (see below).

Since noise is present in the digitized pulses, it is in principle possible to reach an arbitrarily high precision by increasing the number of pulses to average (with no noise present averages of 8-bit data will still yield 8-bit data). However, the limited alignment precision will produce a deformed average pulse that can be described as the convolution of the ideal pulse and the alignment error distribution. In presence of coherent noise the latter distribution is not smooth. This contributes to causing the resulting average pulse shape to be uneven as can be seen for XP2020 in Fig. 1. We also saw that different PMT/base combinations produce different patterns.

Another approach was to expose an XP2020 PMT with a similar base to picosecond light pulses from a frequency doubled 780 nm pulsed dye laser to reproduce light with similar properties as that from LSO in order to investigate the system's impulse response.

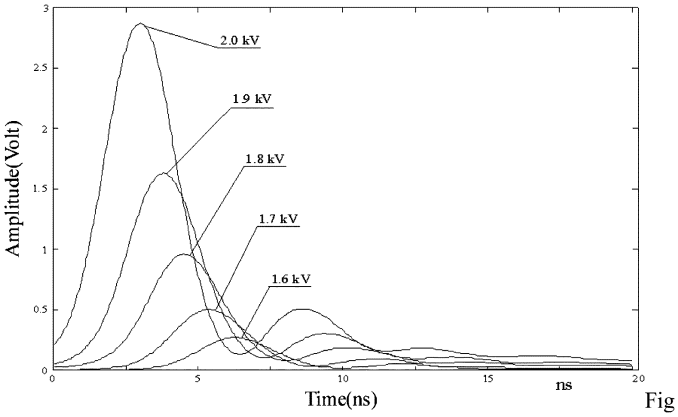

Fig. 2. The impulse response from LSO and XP2020 at different HV-settings.

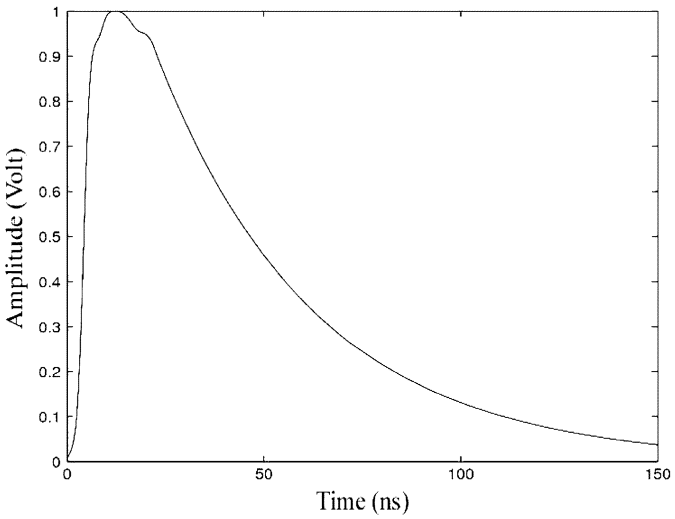

Fig. 3. A reference pulse obtained by convolving an LSO and XP2020 impulse response with an exponential representing the light emission from an LSO crystal.

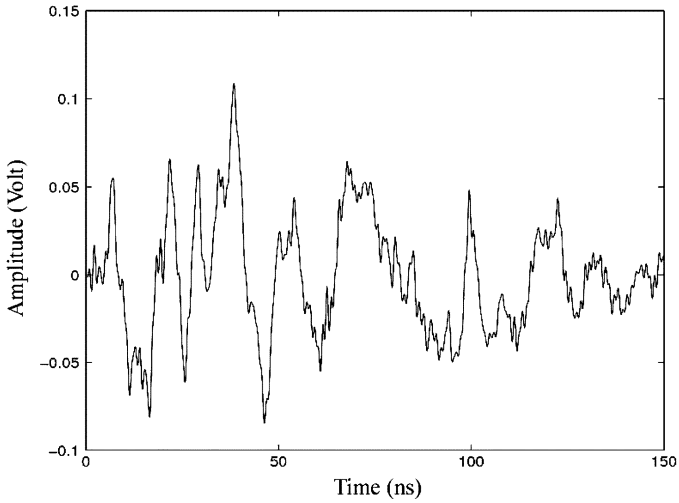

Fig. 4. A "noise" pulse from XP2020.

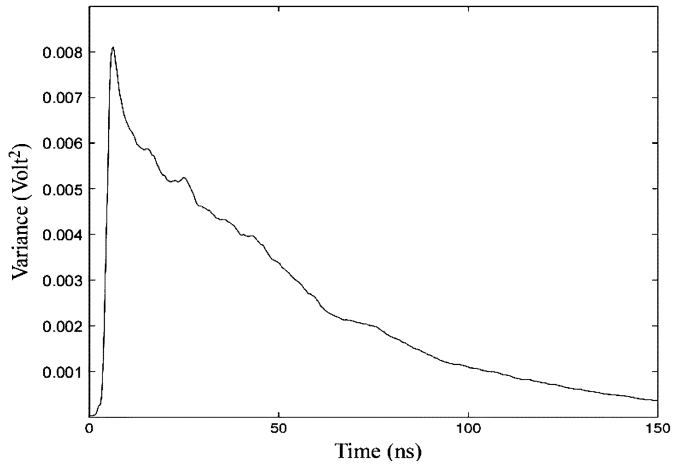

Fig. 5. Noise variance from LSO and XP2020.

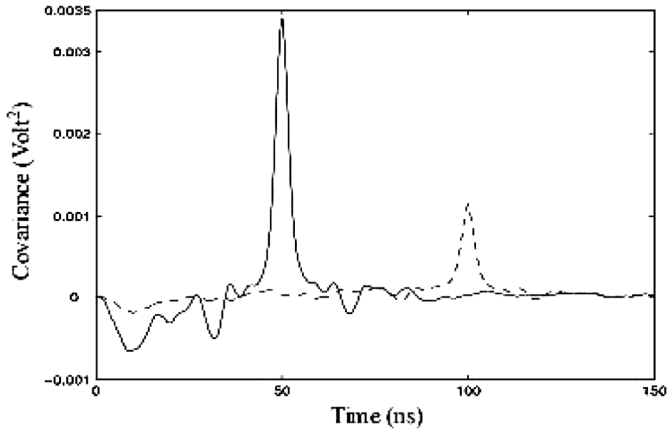

Fig. 6. A noise covariance function for LSO and XP2020, showing the covariance between the pulse amplitude at the time 50 ns and 100 ns and amplitudes at other times.

Fig. 2 shows the impulse response of the combination XP2020 and LSO. We see that the amplitude is increased and the delay is decreased with increased High Voltage settings. The width stays more or less the same. We also see that there is an oscillatory component. The shape of the impulse response is a combination of a Gaussian from the PMT and the dampened oscillatory response from the PMT base circuitry.

Convolving the impulse response with a function describing the light response from the LSO crystal should give us the pulse shape of LSO/PMT combinations (Fig. 3).

When comparing Figs. 1 and 3 we see a similar structure around the maximum. The variations along the trailing edge of XP2020, which are not due to normal noise (they did not disappear with increased sample size), are not present in Fig. 3 since only 20 ns of the impulse response was included in the convolution.

IV. Noise Analysis

Characteristic noise ensembles can be obtained by subtracting the amplitude fitted reference (average) pulse from sample pulses (Fig. 4). By construction the ensemble average of the noise is then zero. Since we have used pulses with approximately constant amplitude we have used the argument leading to expression (3) for optimum timing. Thus, we used expression (2) for amplitude estimation. From this noise we can calculate variances and covariances (Figs. 5 and 6). These are also subject to the alignment error mentioned above. This causes the negative correlation in the early part of Fig. 6 as well as the sharp peak in Fig. 5, since alignment variations add to variance according to the steepness

of the pulse. The variations are significant and will not disappear with improved statistics. The noise variance in Fig. 5 resembles the pulse shape in Fig. 1, which is due to the Poisson character of the PMT noise. The sharp peak is caused by misalignment errors. Some of the variations seen on the trailing edge of the pulse are due to statistics since here increasing the number of samples still improves the smoothness.

The peak in the covariance function tells us how long the influence of a measured value persists. The correlation time, i.e., the width of a rectangle function with the same maximum height, is about 5 ns.

If we express the pulse shape as a convolution of the impulse response of the PMT system, $\mathrm{h(t)}$, (Fig. 2) and the Poisson distributed intensity of the light from the crystal, $\mathrm{q(t)}$, we can calculate the covariance and the variance as [3]:

$$\mathrm{Cov}(t_1, t_2) = \int_{-\infty}^{\infty} q(t) \cdot h(t_1 - t) \cdot h^*(t_2 - t) \cdot dt \tag{7}$$

and

$$\mathrm{Var}(t_1) = \mathrm{Cov}(t_1, t_1) = \int_{-\infty}^{\infty} q(t) \cdot |h(t_1 - t)|^2 \cdot dt. \tag{8}$$

We see that the noise variance and covariance vary substantially along the pulse. This means that the conditions for using matched filters efficiently are not fulfilled. If $\mathrm{q(t)}$ was constant and h real, $\mathrm{Cov}(t, t_1)$ would be completely symmetric around $\mathrm{t_1}$. With an exponential $\mathrm{q(t)}$, which is expected from a scintillator pulse, we get a progressively increasing attenuation with time. This is what we see in Fig. 6. However, the pattern indicates that h is non-zero up to 50 ns from the peak, which is outside the range shown in Fig. 2. $\mathrm{|h(t)|^2}$ is also responsible for the variations in Fig. 5 as well as the variations along the rear slope of the reference pulse (Fig. 1.

V. Pulse Simulations

A simulation model was developed to motivate assumptions and to study different features in the data. Here we used the measured impulse response of the PMT system (see Fig. 2) and an exponential (with the appropriate time constant for LSO, 40 ns [4]) light distribution with Poisson noise. To this we added a small constant white noise, bandwidth limited to 2 GHz. We chose the noise amplitude in order to match the experimental variance and covariance. For the XP 2020 the Poisson noise corresponded to a total of 1 440 photoelectrons in the pulse. With a quantum efficiency of 25% this means about 6 000 photons from the scintillation, a reasonable number considering the crystal dimensions used. A 511 keV gamma incident upon a large crystal produces about 15 000 photons [4]. The quality of the fit was semi-quantitative. It was made by manually scanning the parameter space to keep the computation time at a reasonable level.

The superior timing performance of DCFD compared to DLET, even with pulses even when they were of equal size, was verified with simulated data. It was found to be a statistical effect due to the positive correlation between the trigger and the maximum point (i.e., negative correlation when you subtract these values). A statistical deviation that would often advance the time would also increase the maximum value (both correlation and rise time are about 5 ns). DCFD would then compensate by increasing the efficient threshold and delaying the timing. However, this beneficial effect did not occur if the correlation time was smaller or the slope longer.

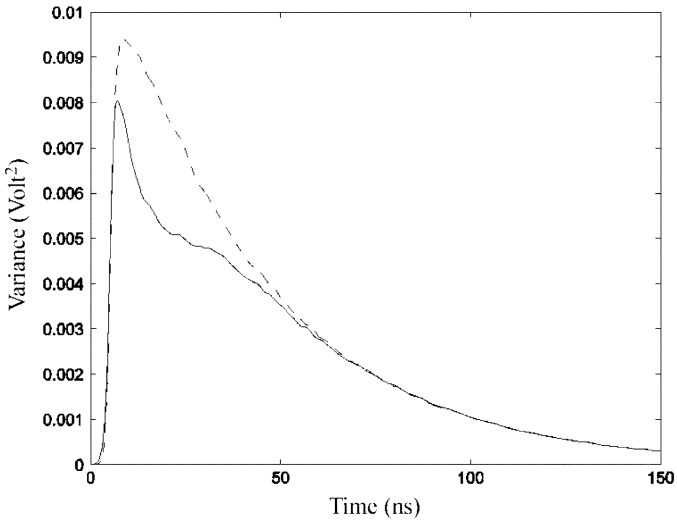

Fig. 7. Noise variance from the simulated data of (LSO-XP2020) with (dashed line) and without (solid line) alignment.

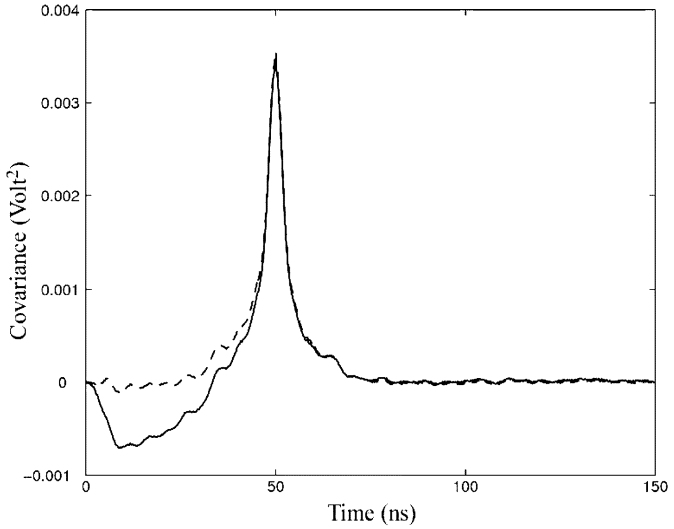

Fig. 8. A noise covariance function from the simulated data of (LSO-XP2020), showing the covariance between the pulse amplitude at the time 50 ns and amplitudes at other times (— not aligned data, - aligned data).

From a large number (16 000) of simulated pulses emitted at the same time we calculated the noise variance with and without alignment with the DCFD method (Fig. 7). From this figure we see the similarity of the variance to the one obtained from the experimental data (Fig. 5). The negative correlation between values in the neighborhood of the pulse maximum and values along the pulse slope is confirmed to be due to the alignment error (Fig. 8) via an erroneous amplitude estimation. That is to say, a pulse where noise causes premature timing will also exaggerate the peak value and thus the amplitude. This will, in turn, cause the values along the slope to be smaller than predicted by the amplitude estimator.

TABLE II
DIGITAL AND ANALOG TIMING RESOLUTION (FWHM)

	XP2020-XP2020 LSO-LSO	*R9779-R9779 LSO-plastic*
Analog	*382 ps*	*290 ps*
Digital (M4)	*351 ps*	*252 ps*

The fine structure around the peak in Fig. 8 is different from Fig. 6 due to fact that the PMT/base combinations were not identical (different $\mathrm{h(t)}$) and only 20 ns of the impulse response were used in the simulation.

VI. RESULTS

A. Timing Resolutions

Table II summarizes the timing resolutions at the FWHM (full width at half maximum) for the digital timing (using method 4 in Table I) when sampling at 2 GHz, and compares these to the result obtained from the analog setup described above. We see that the result from the digital M4 method is 31 ps better than the analog for the XP2020-LSO-LSO combination and 38 ps for the R9779-LSO-plastic combination. Please note the different detector configurations. FWHM was used in the comparison since this was how the analog timing was evaluated. When comparing digital results standard deviation is more convenient.

We calculated the timing of the same set of the data for the (XP2020-XP2020) combination, using DCFD and using cross correlation (M1) with a reference pulse. The result of the cross correlation is in the range of the analog timing while the result from DCFD is few picoseconds better.

The digital M4 method was also compared to the DCFD method using simulated data in order to verify the superiority of the former. The result was a standard deviation of 170 ps and 190 ps, respectively. This is in good agreement with the result obtained experimentally (about 10% improvement).

B. Sample Rate and ADC Precision

After Fourier transforming the average pulse one can evaluate where to apply a frequency limit. The pulse has significant contributions up to 450 MHz. Due to the smoothing effect of the averaging one can assume that the true pulse has a somewhat higher frequency limit. Applying a limit slightly above this point will mostly eliminate noise. By decimating the 20 GHz, after applying the appropriate anti-aliasing filter, we can simulate the effect of lower sample rates. Fig. 9 shows that for both experimental and simulated data nothing significant is lost by sampling with 2 GHz and very little by sampling at 1 GHz (corresponding to 4 points on the less than 5 ns rising edge in Fig. 1).

The standard deviation has also been evaluated using different number of ADC bits for different sampling rates (Fig. 10).

VII. DISCUSSION

If we make some simplifying assumptions, such as that the noise is small, bandwidth limited and uncorrelated and that the pulse amplitude is constant, we can write (1) as:

$$\chi^2 = \sum_i \frac{(Y_i - P_i(t))^2}{\sigma_i^2} \tag{9}$$

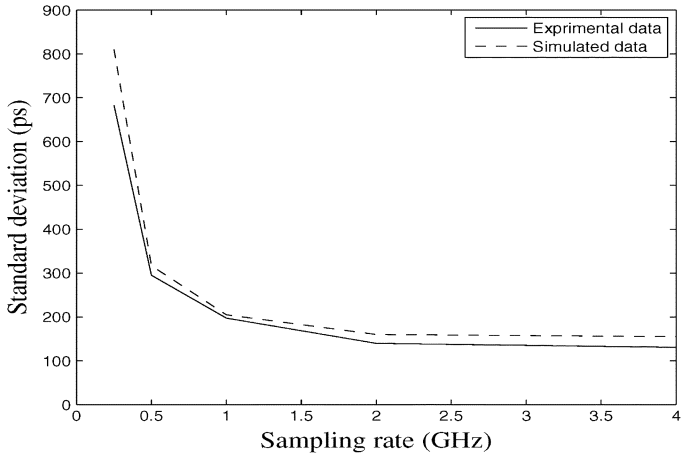

Fig. 9. Dependence of the standard deviation on sample rate for (LSO-XP2020).

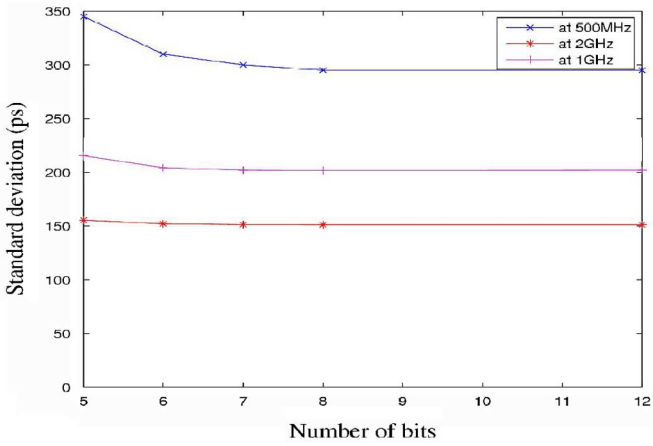

Fig. 10. Dependence of the standard deviation on number of bits for (LSO-XP2020).

where t is the start time and $\mathrm{P_i(t)}$ the value of $\mathrm{P(t)}$ at the i:th sample point.

Minimizing χ^2 with respect to the time gives us the condition:

$$0 = \sum_i \frac{(Y_i - P_i(t)) \cdot P'(t)_i}{\sigma_i^2} = \sum_i \frac{\frac{(Y_i - P_i(t))}{P_i'(t)} \cdot}{\left(\frac{\sigma_i}{P_i'(t)}\right)^2}$$
$$\approx \sum_i \frac{\frac{Y_i - P_i(t)}{P_i'(t_0)} - \Delta t}{\left(\frac{\sigma_i}{P_i'(t_0)}\right)^2}. \tag{10}$$

Here, $\mathrm{P'}$ is the derivative with respect to the start time of the pulse. We have also made a linear Taylor expansion of $\mathrm{P(t)}$ around the approximate start time $(\mathrm{t_0})$. The ratio $(\sigma/\mathrm{P_i'(t_0)})^2$ can be interpreted as the sample variance along the time axis if the noise contribution is small enough [5]. Let us call it σ_t. Solving for $\Delta\mathrm{t}$ gives us:

$$\Delta t \approx \sum_i \frac{(Y_i - P_i(t))/P_i'(t)}{(\sigma_t)_i^2} \Bigg/ \sum_i \frac{1}{(\sigma_t)_i^2} \tag{11}$$

$(\mathrm{Y_i - P_i(t)})/\mathrm{P_i'(t)}$ can be regarded as an estimator of how much the pulse must be displaced to make it intersect the data point

Y_i. It is thus a point estimator for Δt. Expression (11) is then a time variance-weighted estimator using all the available local sample point estimators.

If we assume that the amplitude variances are the same for all sample points along the pulse, the ratio of the inverse variances on the rising and the falling edge would be the ratio of the squares of the slopes. If we incorporate the different numbers of sample points on the two edges, which are proportional to the inverse slopes, we realize that the ratio of the time information from the rising and the falling edge would be the ratio of the slopes (not squared). This means that if we have a symmetric pulse we gain a factor $\sqrt{2}$ if we use both edges for timing. If, on the other hand, the ratio of the slopes are 1:10 we would only gain about 5% ($\approx\sqrt{1.1}-1$). This explains the rather modest gain when using the full statistical treatment.

Although the correlation time is small in this case (about 5 ns, see Fig. 6) it is sufficiently large to involve all sample points along the rising edge, which means that the information from one trigger level and the combined information from all points on the rising edge are not very different. This explains why analogue timing performs as well as it does. The rather poor performance of the cross-correlation method is due to the influence of coherent noise and the fact that the reference pulse we use is slightly larger than the "true" reference pulse, due to the influence of alignment. Without these shortcomings it should have been somewhat better than DCFD.

In Fig. 9 we see that there is a limit beyond which increasing the sample rate does not lead to improved performance. This is in agreement with the Nyquist criteria. However, the bandwidth limit is seldom uniquely defined. There is usually considerable signal power above the 3-dB bandwidth limit. We also have the effect of the digitization, which introduces high frequency noise. We see that increasing the bandwidth compensates errors introduced by the digitization process (Fig. 10), which is expected.

Equation (11) also help us to understand the argument of three sample points on the rising edge (in the introduction). If we have many sample points the combined variance from different sample points will be independent of their exact position (phase independence). After a small phase shift those who gain precision compensate the samples that lose precision. This is not true for a small number of points. The combined variances from two sample points in the beginning and in the end of the leading edge are much larger than one variance at the steepest part. We can also understand that although 3 points are desired on the rising edge we do not need as many as 7 points over a symmetric pulse.

The desired sampling density also depends on the correlation time. Precision is gained by increasing the sample rate as long as it means that more independent measurements are included. A point of diminishing return is reached when the sample distance becomes smaller than the correlation time.

There are different ways to improve the results presented here, but we expect that their effect will be minor. Removing the small but interfering coherent noise is one. Re-measuring the impulse response with an extended time range, using the same PMT/base in the timing set-up, is another way. Further improvement could be achieved by removing the deformation of the reference pulse due to the alignment process. This could be done by de-convolution. Similarly it would be desirable to remove the alignment artifact in the covariance matrix. We can achieve this by using a covariance matrix calculated from expression 7. Improving the processing efficiency would allow a larger number of samples to be used in the analysis. Finally we could improve the model and base the analysis on the fact that we have Poisson statistics (M5 in Table I and expressions 5 and 6).

VIII. Conclusion

The most common digital timing method is to use matched filter techniques to process the sampled data. However, matched filters assume stationary noise. For the case of positron annihilation studied with LSO and XP2020 we have shown that using a method for the non-stationary case derived from "first principles", the least square method, can improve the timing with at least 30 ps. Preliminary measurements indicate that the improvement is better when the correlation time is longer such as when using APDs instead of PMTs. With longer correlation time the consequence of neglecting its influence is, of course, more severe.

Acknowledgment

The authors would like to thank A. Hidvegi for expert help with MatLab calculations and F. Bauer and L. Eriksson for help and discussions regarding PMT properties. The authors would also like to thank M. Bourenenne for allowing the use of the LeCroy oscilloscope and V. Pasiskevicius for access to a femtosecond laser.

References

[1] H. W. Johnson and M. Graham, *High-Speed Digital Design: A Handbook of Black Magic*. Englewood Cliffs, NJ: Prentice-Hall, ch. 1.

[2] A. Boussellham, A. Hidvegi, C. Robson, P. Ojala, and C. Bohm, "A flexible FPGA based acquisition module for high resolution PET camera," in *Proc. IEEE Nuclear and Plasma Sciences Society Real Time Conf.*, Stockholm, Sweden, Jun. 2005.

[3] A. Papoulis, *Probability, Random Variable, and Stochastic Processes*, 4th ed. New York: McGraw-Hill, ch. 9.

[4] A. Nassalski *et al.*, "Comparative study of scintillators for PET/CT detectors," in *Proc. IEEE Nuclear Science Symp. Conf. Rec.*, Oct. 2005, pp. 2823–2829.

[5] A. Pullia and E. Gatti, "Optimal filters with constant-slope crossover and finite width for pulse-timing measurements," *IEEE Trans. Nucl. Sci.*, vol. 49, no. 3, pp. 1170–1176, Jun. 2002.

[6] J. Nissilä, K. Rytsölä, R. Aavikko, A. Laakso, K. Saarinen, and P. Hautojärvi, "Performance analysis of digital positron lifetime spectrometer," *Nucl. Instrum. Methods Phys. Res. A*, vol. A538, pp. 778–789, 2005.

[7] M. A. Nelson, B. D. Roony, D. R. Dinwiddie, and G. S. Brunson, "Analysis of digital timing methods with BaF_2 scintillators," *Nucl. Instrum. Methods Phys. Res. A*, vol. A505, pp. 324–327, 2003.

[8] S.-O. Flyckt and C. Marmonier, Photomultiplier Tubes Principles and Application 2002, ch. 3, Photonis.

[9] A. Pullia, A. Geraci, and G. Ripamonti, "Quasi-optimum η and X spectroscopy based on real-time digital techniques," *Nucl. Instrum. Methods Phys. Res. A*, vol. A439, pp. 378–384, 2000.

[10] A. Fazzi and V. Varoli, "A digital spectrometer for 'optimum' pulse processing," *IEEE Trans. Nucl. Sci.*, vol. 45, no. 3, pp. 843–848, Jun. 1998.

[11] G. Bertuccio, E. Gatti, M. Sampietro, P. Rehak, and S. Rescia, "Sampling and optimum data processing of detector signals," *Nucl. Instrum. Methods Phys. Res. A*, vol. A322, pp. 271–279, 1992.

[12] F. Bauer, M. Aykac, M. Loope, C. W. Williams, L. A. Eriksson, and M. Schmand, "Performance study of the new Hamamatsu R9779 & photonis XP20D0 fast 2″ photomultipliers," in *Proc. IEEE Nuclear Science Symp. Conf. Rec.*, Oct. 2005, vol. 5, pp. 2920–2923.

[13] A. Fallu-Labruyere, H. Tan, W. Hennig, and W. K. Warburton, *Time Resolution Studies Using Digital Constant Fraction Discrimination*. New York: Elsevier, 2001.